Power and spectral analyses in diode-pumped *c*-cut Pbnm Tm:YAP laser

Jacek Kwiatkowski*

Institute of Optoelectronics, Military University of Technology, Warsaw 00-908, Poland
**Corresponding author: jacek.kwiatkowski@wat.edu.pl*

Received April 18, 2020; accepted May 15, 2020; posted online July 24, 2020

Detailed power and spectral analysis of a diode-pumped *c*-cut Pbnm 3 at.% Tm-doped yttrium aluminum perovskite (Tm:YAP) laser in a continuous wave (CW) operation is presented. The laser was experimentally examined in terms of the dependence on the transmittance and radius of curvature of the output coupling mirrors. At room temperature, for an output coupling transmission of 10.8%, the maximum output power of 6.35 W was obtained under a total absorbed pump power of 13.67 W with an optical-to-optical conversion efficiency of 46.5%. The highest slope efficiency of 60.4% was indicated. A detailed spectral analysis was presented. For its dependence on output coupler transmission, the Tm:YAP laser generates wavelengths at approximately 1940 nm or 1990 nm.

Keywords: Tm:YAP laser; mid-infrared; diode-pumped laser; solid-state laser.
doi: 10.3788/COL202018.091401.

Solid-state lasers operating around a 2 μm waveband are in demand, because of their advantage of an eye-safe spectral range, for a variety of applications, such as atmospheric remote sensing[1], medical diagnostics[2,3], and material processing. They are also applicable as pumping sources for the mid-IR region lasers, including Cr:ZnSe[4] and Cr:ZnS[5]. The most attractive and popular laser sources around 2 μm are based on Tm- and Ho-doped materials. Various Tm-doped lasers based on Tm-doped yttrium aluminum garnet (Tm:YAG)[6,7], Tm-doped yttrium lithium fluoride (Tm:YLF)[8,9], Tm-doped potassium lutetium tungstate (Tm:KLuW)[10], Tm-doped scandium silicate (Tm:SSO)[11], Tm-doped potassium yttrium tungstate (Tm:KYW)[12], Tm-doped lutetium aluminum garnet (Tm:LuAG)[13,14], and Tm-doped lutetium silicate (Tm:LSO)[15] crystals have been reported.

Tm:YAP is another interesting gain medium. The thermal and mechanical properties of YAP are similar to those of the common host YAG. Additionally, in comparison with the Tm:YAG crystal, the emission cross section of Tm:YAP (5×10^{-21} cm^2) is more than twice that of the Tm:YAG crystal (2.2×10^{-21} cm^2)[16]. The strong natural birefringence of YAP overwhelms the thermally induced birefringence commonly encountered in media, such as YAG[17]. This feature eliminates thermal depolarization problems, so Tm:YAP lasers can generate linearly polarized output radiation with a high polarization extinction ratio desirable for pumping, e.g., YLF hosts. In addition, beneficial to the cross-relaxation process that occurs between adjacent Tm ions[18], quasi-three-level Tm-based systems offer a high efficiency comparable to Nd-doped laser systems. The Tm:YAP possesses a strong absorption peak near 793 nm, making it possible to pump with very popular and relatively cheap AlGaAs high-power laser diodes (LDs).

High power and efficiency Tm:YAP lasers in various configurations have been widely investigated in recent years[19–23]. The properties of Tm:YAP depend on the crystal orientation. From the references cited above, Tm:YAP lasers generate output wavelengths around 1.94 and 1.99 μm. In the Tm:YAP crystal, the strong peak at 1.94 μm dominates the laser emission for E||c at Pnma polarization, whereas, for E||c at Pbnm, two significant emission peaks are located at 1.94 and 1.99 μm. The transformation between the two coordinate systems is given by

$$(a, b, c)\,\mathrm{Pbnm} \leftrightarrow (c, a, b)\,\mathrm{Pnma}. \tag{1}$$

To achieve the expected laser output wavelength or maximize the laser gain to obtain a high-efficiency laser output, the axis cut of the laser crystal must be known. Owing to the quasi-three-level nature, most of the Tm lasers are blue-shifted as the output coupler (OC) transmission or the cavity losses increase.

The preferential free-running laser wavelength at room temperature for different axis cuts of Tm:YAP under various cavity output mirror transmissions was theoretically analyzed[24]. However, no detailed reports exist about experimental verification of this phenomenon. In this Letter, energetic and spectral analysis of a diode-pumped *c*-cut at Pbnm notation 3 at. % Tm:YAP laser in a continuous wave (CW) operation is presented. Additionally, the obtained slope efficiencies in the developed laser are one of the highest ever reported.

A Tm:YAP laser single-pass end-pumped by a fiber-coupled LD at 793 nm with a core diameter of 200 μm and a numerical aperture of 0.22 is shown in Fig. 1. To achieve the highest efficiency of the pumping scheme, in the preliminary experiments the LD emission was temperature tuned to the absorption peak of Tm in YAP. A 1:2 coupling optics system was employed to focus the pump

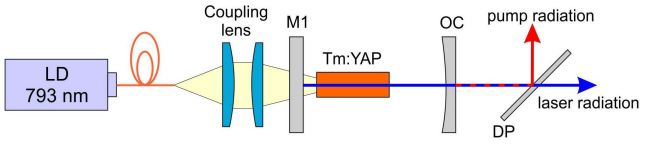

Fig. 1. Experimental setup of the diode-pumped Tm:YAP laser.

light into the gain material. The pump beam was focused using a pair of plano-convex lenses with focal lengths of 22 mm and 44 mm, respectively, which resulted in a pumping beam diameter of approximately 400 μm positioned in the center of the crystal.

The *c*-cut (Pbnm) Tm:YAP brick at 3 mm × 3 mm × 8 mm and a doping concentration of 3 at.% was used as an active medium. The crystal facets were polished plane and anti-reflection (AR) coated at 793 nm and 1930–2000 nm wavelengths, respectively. The crystal was then wrapped with indium foil and tightly mounted in a water-cooled copper heat sink for better thermal contact at a constant water temperature of 17°C.

In the dependence of the OC radius of curvature, the Tm:YAP laser resonator physical cavity lengths changed from 47 to 55 mm. The input cavity mirror M1 was flat with high reflectivity in the wavelength range of 1.92 to 2.1 μm and high transmission at 793 nm. Considering the transmission losses on the coupling lenses and dichroic mirror M1, more than 90% of the available diode pump power was incident onto the crystal, which was 18.16 W, and the Tm:YAP crystal absorbed 75% of this pump power.

The plano-concave mirror OC of a different radius of curvature (R_{OC}) and transmission (T_{OC}) was used as the OC. For the experiment, OCs of radii of curvature at 100, 200, 300, and 400 mm were utilized. The calculated transverse electromagnetic mode (TEM_{00}) average beam diameters in the Tm:YAP crystal were approximately

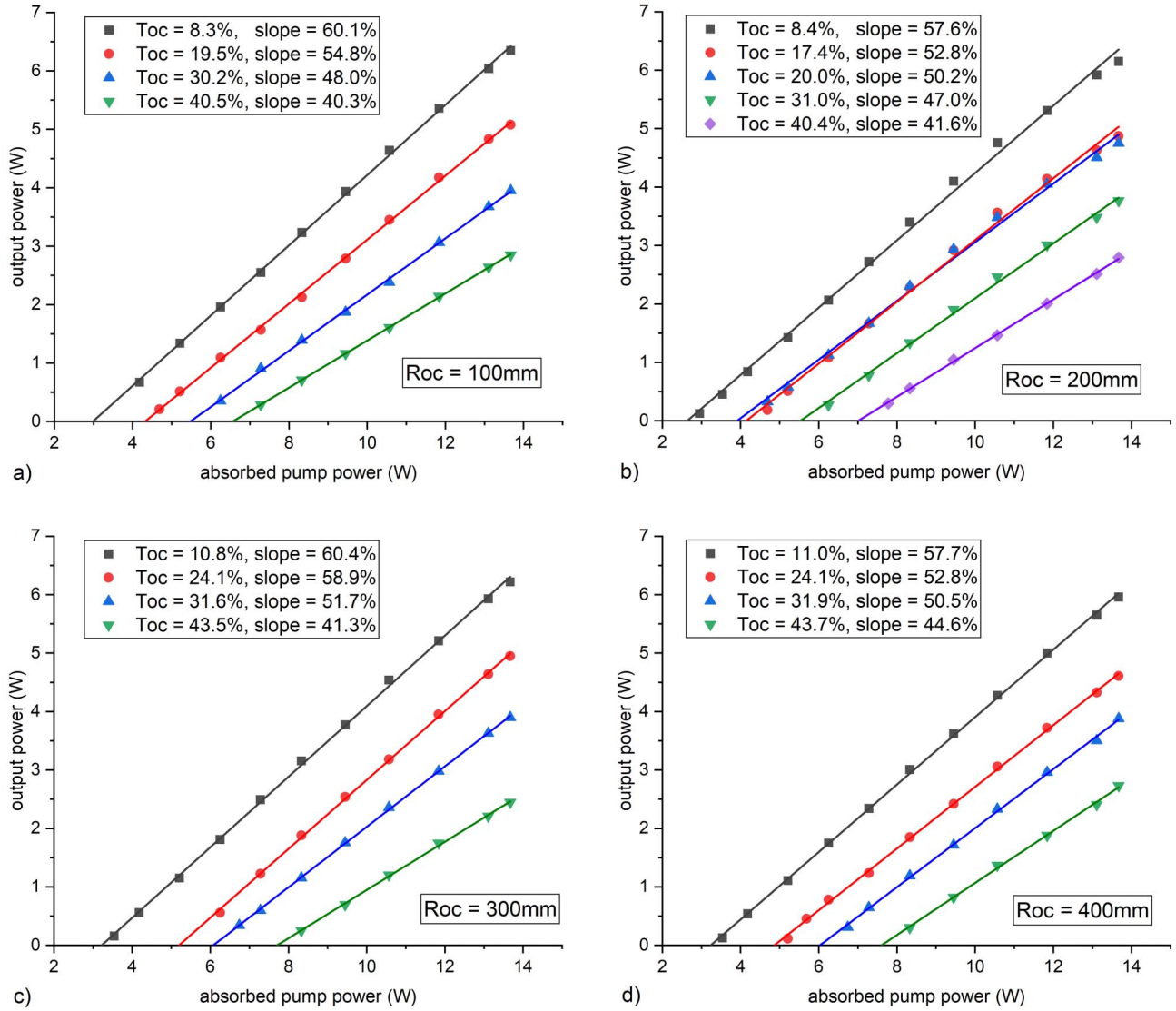

Fig. 2. Output powers of the Tm:YAP laser under different output mirror transmissions as a function of the absorbed pump power for a radius of curvature of (a) 100 mm, (b) 200 mm, (c) 300 mm, and (d) 400 mm. The results of a linear fit and the calculated slope efficiencies are presented in the graphs.

260, 330, 370, and 400 μm, respectively. With the 400 μm pump spot diameter inside the crystal, different overlap efficiencies of the pump-to-Tm-resonator mode were achieved. Unabsorbed by the laser crystal, pump power was reflected by the dichroic beam splitter plate (DP) [high reflection (HR) at 793 nm and AR at 1.92–2.0 μm at a 45° angle of incidence].

The diode-pumped Tm:YAP laser was studied during CW operation. The output power and spectral characteristics with different OCs were investigated in detail, with the results shown in Figs. 2 and 3, respectively. To optimize the output power, the distance from the collimating lens to the Tm:YAP crystal and the physical cavity length were adjusted for each OC radius of curvature.

The output power increased linearly with an increase in the absorbed pump power for each case. For the maximum CW absorbed pump power of 13.67 W, with an OC transmittance of $T_{OC} = 8.3\%$ and radius of curvature of $R_{OC} = 100$ mm, the laser generated output power was as high as 6.35 W. This result corresponds to a slope efficiency of 60.1% and maximum optical-to-optical conversion efficiency of 46.5% with respect to the absorbed pump power [Fig. 2(a)]. The corresponding slope efficiency with respect to the incident pump power was 45.8%. However, the highest slope efficiency of 60.4% with respect to the absorbed pump power was achieved for the laser based on the OC transmittance of $T_{OC} = 10.8\%$ and radius of curvature of $R_{OC} = 300$ mm [Fig. 2(c)].

The output free-running spectra of the Tm:YAP laser were measured with an AQ6375 optical spectrum analyzer made by Yokogawa. No significant differences in the output laser wavelengths were observed in relation to the values of the OC R_{OC}.

Because of the Tm:YAP laser levels feature, the operating wavelengths were shifted based on the output coupling transmittances. The change in the OC resulted in a change in the intracavity laser intensity. This behavior, in turn, changed the pump absorption of the Tm:YAP crystal because pump absorption is a function of laser intensity. With the same pump power, a lower T_{OC} resulted in higher intracavity intensity and an increase in pumping efficiency. An increase in the OC transmission causes the laser to operate at shorter wavelengths. Figure 3 shows that the output laser wavelengths were centered around 1990 nm only for the OC transmittances lower than 17.4%.

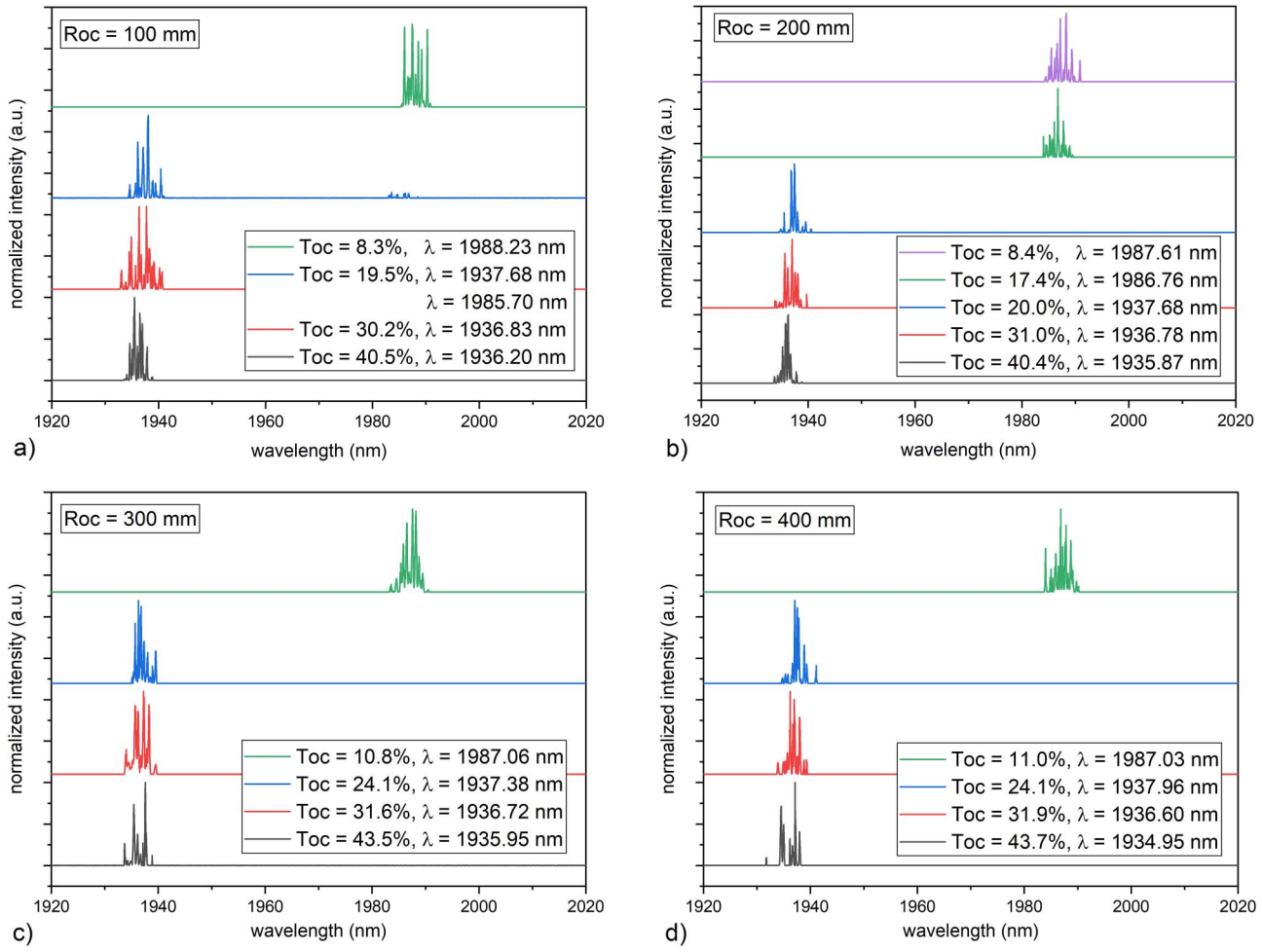

Fig. 3. Output spectra from the Tm:YAP laser in CW operation under different output mirror transmissions for a radius of curvature of (a) 100 mm, (b) 200 mm, (c) 300 mm, and (d) 400 mm.

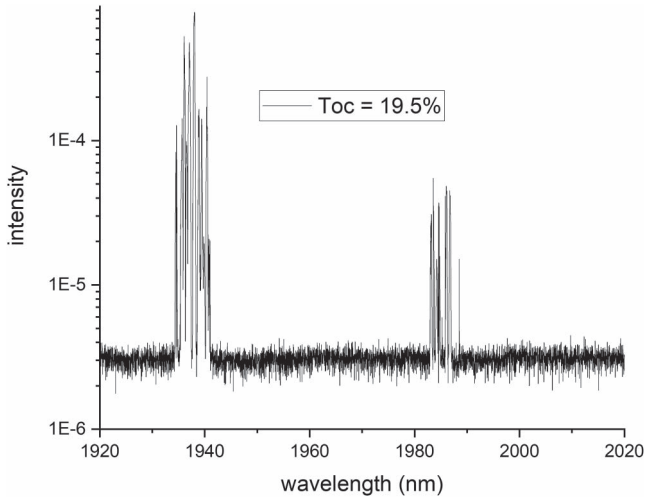

Fig. 4. Output spectrum from the Tm:YAP laser for the output mirror transmission of 19.5% and the radius of curvature of 100 mm shown on a logarithmic scale.

For the lowest OC, the developed laser characterized the highest output power. Unfortunately, this is an undesirable feature for the need to develop an efficient laser system that generates radiation with a wavelength of 1940 nm, which can be used as a pumping system for the Ho:YLF active medium.

For the higher OC transmittances, the generated laser wavelengths shifted to around 1940 nm, reaching 1935 nm for a T_{OC} of 43.7%. For the OC, the $R_{OC} = 100$ mm and T_{OC} of 19.5% Tm:YAP laser generated simultaneously two wavelengths. To check the two wavelengths generation intensity contrast at 1937.68 nm and 1985.70 nm, the spectral characteristic for $T_{OC} = 19.5\%$ on a logarithmic scale is presented in Fig. 4. To the best of our knowledge, this phenomenon was experimentally observed for the first time. We assume that applying the out-coupling transmission of approximately 18% to 19% can force simultaneous generation at two laser wavelengths of the same intensity.

Summarized experimental data of slope and optical-to-optical efficiencies with respect to the absorbed pump power are listed in Table 1. Also included in the table are the maximum output powers and generated wavelengths from the Tm:YAP laser obtained versus the different transmittances of the OC T_{OC} and radius of curvature R_{OC}.

The Tm:YAP laser generated beam spatial structure was measured with a pyroelectric NanoScan, a scanning-slit laser beam profiler that uses a lens with a focal length of $f = 500$ mm. Measurements of the M^2 parameter were performed for OCs with a radius of curvature of $R_{OC} = 400$ mm and two output transmittances of 11.0% and 43.7%, for which the laser generated radiation with the largest (1987.03 nm) and smallest (1934.95 nm) wavelengths. Based on the changes in the diameter of the laser beam after passing through the focusing lens and by fitting

Table 1. Experimental Results of the Tm:YAP Laser in CW Operation.

Radius of Curvature (mm)	Transmission of OC (%)	Maximum Output Power (W)	Slope Efficiency (%)	Optical-to-Optical Efficiency (%)	Laser Wavelength (nm)
100	8.3	6.35	60.1	46.5	1988.23
	19.5	5.08	54.8	37.2	1937.68; 1985.70
	30.2	3.95	48.0	28.9	1936.83
	40.5	2.85	40.3	20.8	1936.20
200	8.4	6.15	57.6	45.0	1987.61
	17.4	4.87	52.8	35.6	1986.76
	20.0	4.75	50.2	34.7	1937.68
	31.0	3.76	47.0	27.5	1936.78
	40.4	2.79	41.6	20.4	1935.87
300	10.8	6.22	60.4	45.5	1987.06
	24.1	4.95	58.9	36.2	1937.38
	31.6	3.90	51.7	28.5	1936.72
	43.5	2.45	41.3	17.9	1935.95
400	11.0	5.96	57.7	43.6	1987.03
	24.1	4.61	52.8	33.7	1937.96
	31.9	3.88	50.5	28.4	1936.60
	43.7	2.73	44.6	20.0	1934.95

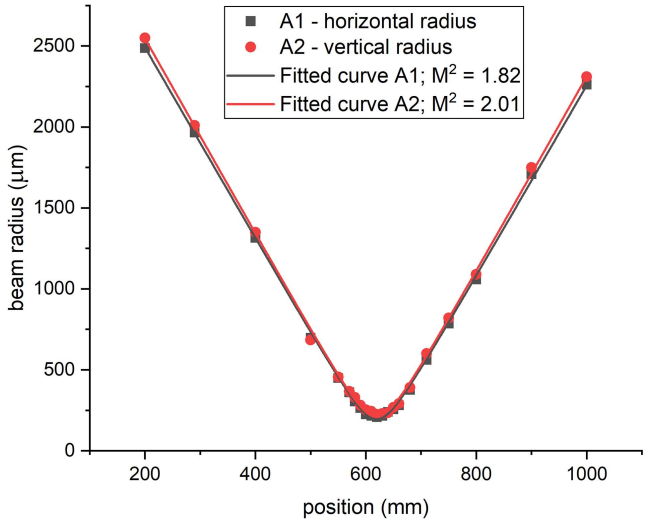

Fig. 5. Measurement results of the Tm:YAP laser beam quality for the OC of 11.0% transmittance.

a Gaussian beam propagation expression to the experimental data, the basic parameters of the laser beam in the perpendicular planes A1 and A2 were determined. The results of the measurements of the M^2 parameter for the two OCs are presented in Figs. 5 and 6.

The beam profile in the 2D and 3D dimensions recorded by the pyroelectric NanoScan profiler for the maximum output power is shown in Fig. 7.

In conclusion, a high-efficiency Tm:YAP laser was demonstrated. By optimizing the LD emission to the absorption peak of Tm in YAP and the overlap efficiency of the pump-to-Tm-resonator mode, we achieved the highest slope efficiency of 60.4% with respect to the absorbed pump power. For the maximum absorbed pump power of 13.67 W (incident pump power of 18.16 W), the Tm:YAP laser yielded 6.35 W output power. In the spectral analysis, the increase in transmission of the OC resulted in the

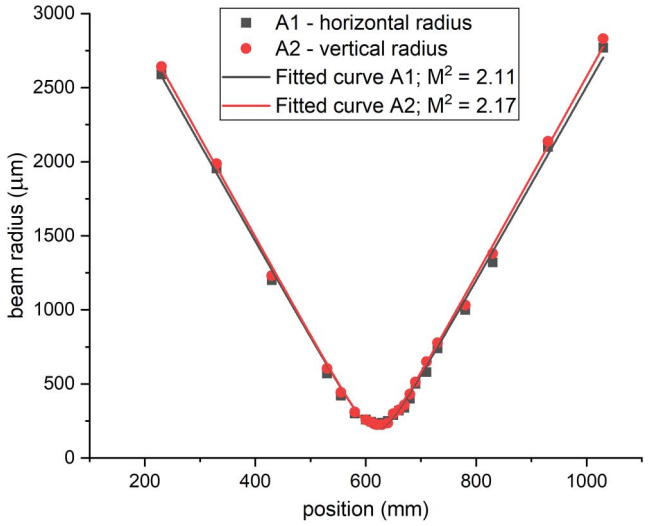

Fig. 6. Measurement results of the Tm:YAP laser beam quality for the OC of 43.7% transmittance.

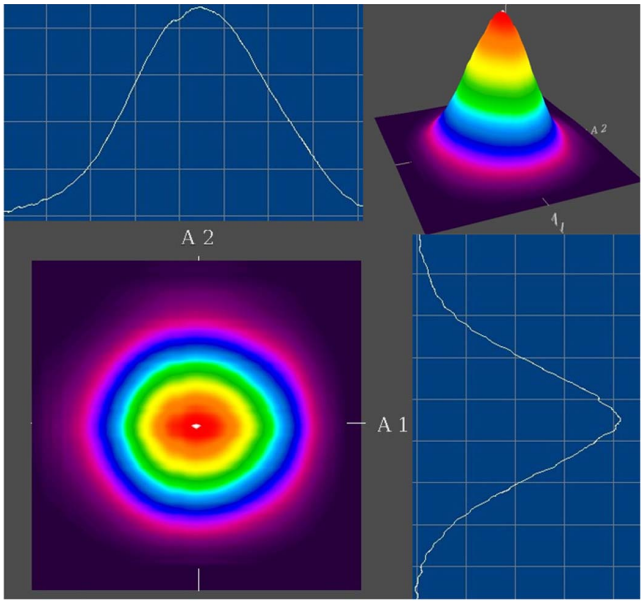

Fig. 7. Diode-pumped Tm:YAP laser generated beam spatial distribution recorded for the output coupler transmittance of 11.0%.

generation of a laser for lower wavelengths. To the best of our knowledge, simultaneous generation of two laser wavelengths in the Tm:YAP laser was presented for the first time. These experimental results offer guidelines for choosing the Tm:YAP laser parameters for achieving the expected spectral and energetic characteristics of the developed laser system.

This work was supported by the Ministry of National Defense of Poland (No. GBMON/13-992/2018/WAT).

References

1. T. Refaat, U. Singh, J. Yu, M. Petros, R. Remus, and S. Ismail, Appl. Opt. **55**, 4232 (2016).
2. H. Jelínková, P. Koranda, J. Sulc, M. Nemec, P. Cerny, and J. Pasta, Proc SPIE **6871**, 68712N (2008).
3. V. Serebryakov, É. Boĭko, A. Kalintsev, A. Kornev, A. Narivonchik, and A. Pavlova, J. Opt. Technol. **82**, 781 (2015).
4. Y. F. Dai, Y. Y. Li, X. Zou, Y. J. Dong, and Y. X. Leng, Laser Phys. Lett. **10**, 105816 (2013).
5. Y. Dai, Y. Li, X. Zou, B. Jiang, Y. Hang, and Y. Leng, Opt. Laser Technol. **57**, 202 (2014).
6. J. Zhang, F. Schulze, K.F. Mak, V. Pervak, D. Bauer, D. Sutter, and O. Pronin, Laser Photon. Rev. **12**, 1700273 (2018).
7. X. F. Zhang, Y. T. Xu, C. M. Li, N. Zong, J. L. Xu, Q. J. Cui, Y. F. Lu, Y. Bo, Q. J. Peng, and D. F. Cui, Chin. Phys. Lett. **25**, 3673 (2008).
8. Ł. Gorajek, J. K. Jabczyński, W. Żendzian, J. Kwiatkowski, H. Jelinkova, J. Sulc, and M. Nemec, Opto-Electron. Rev. **17**, 309 (2009).
9. R. Faoro, M. Kadankov, D. Parisi, S. Veronesi, M. Tonelli, V. Petrov, U. Griebner, M. Segura, and X. Mateos, Opt. Lett. **37**, 1517 (2012).
10. M. Segura, M. Kadankov, X. Mateos, M. C. Pujol, J.J. Carvajal, M. Aguiló, F. Díaz, U. Griebner, and V. Petrov, Opt. Express **20**, 3394 (2012).

11. T. L. Feng, K. J. Yang, S. Z. Zhao, W. C. Qiao, J. Zhao, D. C. Li, G. Q. Li, T. Li, L. H. Zheng, J. Xu, Q. G. Wang, X. D. Xu, and L. B. Su, Opt. Commun. **336**, 20 (2015).
12. M. Gaponenko, N. Kuleshov, and T. Südmeyer, Opt. Express **22**, 11578 (2014).
13. L. Wang, C. Gao, M. Gao, L. Liu, and F. Yue, Appl. Opt. **52**, 1272 (2013).
14. C. T. Wu, Y. L. Ju, and Y. Z. Wang, Laser Phys. **23**, 105810 (2013).
15. T. L. Feng, S. Z. Zhao, K. J. Yang, G. Q. Li, D. C. Li, J. Zhao, W. C. Qiao, J. Hou, Y. Yang, J. L. He, L. H. Zheng, Q. G. Wang, X. D. Xu, L. B. Su, and J. Xu, Opt. Express **21**, 24665 (2013).
16. S. A. Payne, L. L. Chase, L. K. Smith, W. L. Kway, and W. F. Krupke, IEEE J. Quantum Electron. **28**, 2619 (1992).
17. W. Koechner, *Solid-state Laser Engineering* (Springer, 2013).
18. G. Rustad and K. Stenersen, IEEE J. Quantum Electron. **32**, 1645 (1996).
19. J. Li, S. H. Yang, H. Y. Zhang, D. X. Hu, and C. M. Zhao, Laser Phys. Lett. **7**, 203 (2010).
20. U. Sheintop, E. Perez, and S. Noach, Appl. Opt. **57**, 1468 (2018).
21. H. Zhang, J. He, Z. Wang, J. Hou, B. Zhang, R. Zhao, K. Han, K. Yang, H. Nie, and X. Sun, Opt. Mater. Express **6**, 2328 (2016).
22. J. Hou, B. Zhang, J. He, Z. Wang, F. Lou, J. Ning, R. Zhao, and X. Su, Appl. Opt. **53**, 4968 (2014).
23. B. Cole, L. Goldberg, and A. D. Hays, Opt. Lett. **43**, 170 (2018).
24. G. Li, H. Liu, F. Lu, X. Wen, Y. Gu, and Y. Wang, Appl. Opt. **53**, 4987 (2014).